HIV Antiretroviral Therapy Drugs Induce Premature Senescence and altered Physiology in HUVECs

Justin Cohen, **Luca D'Agostino**, **Ferit Tuzer**, and **Claudio Torres**[*]

Department of Pathology and Laboratory Medicine, Drexel University College of Medicine, Philadelphia, Pennsylvania, USA

Abstract

Developments in medicine have led to a significant increase in the average human lifespan. This increase in aging is most readily apparent in the case of HIV where antiretroviral therapy has shifted infection from a terminal to a chronic but manageable disease. Despite this advance, patients suffer from co-morbidities best described as an accelerated aging phenotype. A potential contributor is cellular senescence, an aging-associated growth arrest, which has already been linked to other HIV co-morbidities such as lipodystrophies and osteoporosis in response to antiretroviral drugs. We have previously demonstrated that astrocytes senescence in response to antiretroviral drugs. As endothelial cells play a critical role regulating the blood brain barrier (BBB) and senescence could severely impact barrier permeability, we investigate the role of a commonly used combination of HIV reverse transcriptase inhibitors on the senescence program of human umbilical vein endothelial cells (HUVECs). Our studies indicate that HUVECs underwent premature senescence associated with inflammation, oxidative stress and altered eNOS activation. Treated cells had detrimental paracrine effects on astrocytes including paracrine senescence, suggesting that senescent HUVECs could influence astrocytes, which line the other side of the BBB. These results may have implications for HIV-associated neurocognitive disorders (HAND), a set of neurological deficits.

Keywords

[*]Corresponding author at: Department of Pathology and Laboratory Medicine, Drexel University College of Medicine, Philadelphia, 245 N.15th Street, New College Building MS 435, Philadelphia, Pennsylvania 19102, USA. Tel: +1 215-762-1783; fax: +1 215-762-3978 cat36@drexel.edu (Claudio Torres).

Conflicts of interest
The authors have declared no conflict of interest.

1. Introduction

Following the emergence of highly active antiretroviral therapy (HAART), HIV infection has converted from a critical, fatal illness to a chronic but manageable condition (Bhatia et al., 2012). The HIV-infected population is consequently aging, and it had been projected that by 2015 more than 50% of the HIV-infected population in the United States would be 50 years of age and older (Effros et al., 2008). While not quite 50% as of this writing, the population is on track to reach this percentage in a few years and is even estimated to reach 70% by 2030 (Negredo et al., 2017). Although this increased lifespan is modern medical marvel, aging is a significant risk factor for disease (Niccoli and Partridge, 2012) and HIV patients experience a variety of ailments experienced in the elderly. HIV patients are therefore considered to undergo accelerated aging (Capeau, 2011). One such complication is a series of neurological problems collectively known as HIV-associated neurocognitive disorders (HAND) (Heaton et al., 2010). HAND is classified into several categories with the most severe being HIV-associated dementia (HAD) down to mild neurocognitive disorder (MND) and asymptomatic neurocognitive impairment (ANI). While the prevalence of HAD in the post-HAART era has decreased in HIV-infected patients, ANI and MND have increased (Heaton et al., 2010). The persistence of these neurological problems such as cognitive impairment, motor dysfunction, speech and behavioral changes in HIV-infected patients remain a major public health issue and the identification of mechanisms involved may lead to potential treatments (Saylor et al., 2016).

One possible contributor to HAND could be the antiretroviral drugs themselves because even though these compounds are beneficial in their suppression of HIV, HAART drugs have been demonstrated to cause neuronal damage in the central nervous system (CNS) (Akay et al., 2014). These complications suggest that cells may undergo a great deal of stress in response to HAART drugs, leading to HIV co-morbidities. Indeed, numerous cell types including adipocytes, mesenchymal stem cells, smooth muscle and endothelial cells have been associated with HIV comorbidities ranging from osteoporosis to laminopathies in response to HAART drug treatment (Afonso et al., 2015; Afonso et al., 2017; Auclair et al., 2014; Caron et al., 2008; Hernandez-Vallejo et al., 2013). The above studies as well as two others involving HAART drug associated dysfunction in astrocytes and fibroblasts (Cohen et al., 2017; Nacarelli et al., 2016) can be linked together through the premature induction of cellular senescence, an aging associated growth arrest accompanied by various phenotypic changes (van Deursen, 2014). Senescent cells increase with age in tissues and have been associated with diseased tissues. These discoveries have led to the proposal of senescent cells as contributors to disease (Jeyapalan and Sedivy, 2008; Munoz-Espin and Serrano, 2014). Given that premature senescence of CNS cells has been linked to neurodegenerative disorders such as Alzheimer's and Parkinson's disease (Bhat et al., 2012; Chinta et al., 2018; Turnquist et al., 2016), it is likely that CNS senescence could also be linked to HAND.

One possible way CNS senescence could contribute to HAND is at the blood brain barrier (BBB), a selective semipermeable membrane responsible for preventing circulating blood from penetrating the CNS. Compounds instead infiltrate the brain based on their polarity and size (Correale and Villa, 2009). The BBB is primarily composed of perivascular pericytes, astrocytic endfeet and endothelial cells. Since the BBB plays an essential role in

neurological health by preventing unwanted compounds from entering the CNS, dysfunction associated with endothelial cell senescence is a likely contributor to HAND. Endothelial cells have previously been demonstrated to undergo premature senescence in response to external stressors such as TNFα, H_2O_2 and even HIV gp120 (Hijmans et al., 2018; Khan et al., 2017; Rojas et al., 2017). We therefore hypothesize that the antiretroviral reverse transcriptase inhibitors tenofovir (TDF) and emtricitabine (FTC) constitute an HIV-associated stressor that prematurely may induce senescence in human umbilical vein endothelial cells (HUVECs) and alter their functional physiology. We propose that this dysfunction could be a contributor to HAND.

2. Materials & methods

2.1. HUVEC cell culture and drug treatments

Human umbilical vein endothelial cells (HUVECs) were cultured at 37°C, 5% CO2 in endothelial cell medium (ECM) supplemented with 10% fetal bovine serum, growth supplement, and penicillin/streptomycin all obtained from ScienCell Research Laboratories (Carlsbad, CA). Cells were cultured in 10 cm^2 plates until they reached ~80% confluence before passaging. Before treatment, cells at 5 to 7 population doublings were plated in the indicated plates for each experiment below at one-half standard density. HUVECs were chronically treated twice over a one-week period with either 0.2% ddH$_2$O as a vehicle control or 10 μg/mL of the HAART drugs TDF and FTC dissolved in ddH$_2$O. The vehicle or HAART drugs were added to the ECM before addition to the cells. During the treatment, media was only changed when the second round of treatments occurred which was 3 days after the initial treatment. The control cells were treated with the vehicle in parallel to TDF-FTC treatment. HAART drugs were provided by the NIH AIDS Reagent Program.

2.2. Human astrocyte cell culture

Human astrocytes were cultured at 37°C, 5% CO2 in human astrocyte medium (HAM) supplemented with 2% fetal bovine serum, growth supplement, and penicillin/streptomycin all obtained from ScienCell Research Laboratories (Carlsbad, CA). Cells were cultured in 10cm^2 plates until they reached ~80% confluence before passaging. Astrocytes at 4 population doublings were plated in the indicated plates below at one-half standard density for paracrine experiments.

2.3. p38MAPK inhibition

In 12-well plates, prior to the addition of HAART drugs, HUVECs were pre-incubated with ECM containing 10 μM of the p38MAPK inhibitor SB 203580 (Enzo Life Sciences, Farmingdale, NY) for 2 hours. After this period the HAART drugs were added to the media without removing SB 203580. This was repeated 3 days after the initial treatment. Outcomes were determined one week after initial treatment.

2.4. Senescence-associated β-galactosidase activity assay

In 12-well plates, senescence-associated beta-galactosidase (SA β-gal) staining was performed as previously described (Dimri et al., 1995). Briefly, following exposure to the HAART drug combinations or DMSO, astrocytes were fixed in 2% formaldehyde/0.2%

glutaraldehyde for 3 minutes and stained for SA β-gal activity overnight. The cells were counted and positive (blue) cells were expressed as a percentage of the total. At least 200 cells were counted per well.

2.5.   Immunoblotting

In 6 cm^2 plates, following indicated treatment times, HUVECs were lysed in RIPA buffer. Western blot analysis was performed under standard conditions using 15 μg of total cell proteins. Membranes were probed for antibodies against lamin B1 (ab16048, polyclonal, Abcam, Cambridge, MA), phosphorylated (3033) and total p65 (3034) both polyclonal, (Cell Signaling Technology, Danvers, MA), HMGB2 (LS-B4355**(3D2)**, monoclonal, LSBio, Seattle, WA), phosphorylated (9570s) and total eNOS (9572s) both polyclonal, (Cell Signaling Technology, Danvers, MA), β-actin (A00702 **(2D1D10)**, monoclonal, Genscript, Piscataway, NJ). Clone numbers are in bold. For eNOS measurements, HUVECs were treated with 100 μM ATP for one min prior to lysis.

2.6.   HMGB2 Secretion Quantification

HUVECs on round glass slides in 12-well plates were fixed for 30 min. with 4% paraformaldehyde in PBS. After fixation, cells were washed for washed 3X in PBS for 5 min. each before permeabilization with 0.2% Triton X-100 in PBS for 15 min. Cells were washed 3X in PBS for 3 min. each before blocking for 2 hours at room temperature with 5% goat serum in PBS. Cells were then incubated overnight in a humidified chamber at 4°C with anti-HMGB2 (LSBio, Seattle, WA). Slides were washed 3X for 5 min. each in PBS before incubation for 1 hour in the dark at room temperature with the secondary antibody anti-mouse Alexa Fluor 555 (Invitrogen, Carlsbad, CA). Cells were then washed 3X for 5 min. each in 1X PBS before incubation in the dark for 10 min. at room temperature with DAPI at 1:5000 in PBS. Lastly, cells were washed 3X for 3 min. each with ddH$_2$O before mounting on glass slides with Fluoromount Mounting Medium (Sigma-Aldrich, Darmstadt, Germany). Cells were visualized using an Olympus BX61 fluorescence microscope coupled with a Hamamatsu ORCA-ER camera and using Slide Book 4 software version 4.0.1.44 (Intelligent Innovations, Inc.; Denver, CO). HMGB2 secreting cells were blindly counted by a laboratory member who did not know the conditions and at least 200 cells were counted per coverslip at 40X magnification.

2.7.   Total cellular ROS, mitochondrial ROS and lysosomal mass

In 12 well plates, determination of total cellular reactive oxygen species (ROS), mitochondrial ROS and lysosomal mass were made using flow cytometry as previously described (Cohen et al., 2017). In brief, total cellular ROS were detected by incubating cells with 10 μM 2′7′ dichlorofluoroscein diacetate (DCF-DA; Sigma-Aldrich, St. Louis, MO) in 1% fetal bovine serum-supplemented MEM and washing twice with Krebs Ringer phosphate glucose buffer following incubation. All other compounds were washed with PBS. Mitochondrial superoxide levels were assayed by incubating the cells with 5 μM Mito-Sox Red (Molecular Probes Waltham, MA). Lysosomal mass was evaluated by incubating the cells with 50 nM Mito-tracker Green (Molecular Probes, Waltham, MA). For the previous analyses, incubation was performed at 37 °C in 5% CO2 for 30 min. Cells were collected in

0.25% trypsin-EDTA with complete medium. Cells were analyzed by flow cytometry using a Guava EasyCyte Mini and the Guava Express Plus program (Guava Technologies, City State). Acquisitions involved 5000 events.

2.8. Nitric oxide measurement

In 12-well plates, intracellular nitric oxide (NO) assessments were made by flow cytometry. HUVECs were incubated for 30 min in complete endothelial cell media with 5 μM of 4-Amino-5-Methylamino-2',7'-Difluorofluorescein Diacetate (DAF-FM) and 100 μM ATP at 37 °C in 5% CO_2. Cells were washed with PBS and then incubated with fresh endothelial cell media for 15 min. Cells were collected in 0.25% trypsin-EDTA with complete medium and analyzed by flow cytometry using a Guava EasyCyte Mini and the Guava Express Plus program (Guava Technologies, City State). Acquisitions involved 5000 events.

2.9. Cytokine array

In 10 cm^2 plates, following the end of the one-week treatment period, HUVECs were incubated with serum-free MCDB105 media (Sigma-Aldrich, Darmstadt, Germany). After a 24-hour incubation period, media was collected and cells were trypsinized and counted to determine the cell number for normalization. Human cytokine array C5 (RayBiotech, Norcross, GA) was used to evaluate secreted inflammatory factors in the conditioned media according to the company's protocol. The intensity of the signal on the array membranes was quantified by densitometry using ImageJ software and normalized to cell number. The HAART drug treated values were then set as relative to vehicle control values. Samples that had no change in expression due to levels being undetectable from background were set to 1.

2.10. ELISA assays

IL-6 and IL-8 detection was performed via their respective Human Quantikine ELISA kit (R&D Systems, Minneapolis, MN) according to the product manual using conditioned media as described above. Absorbance was measured at 450 nm.

2.11. Paracrine effect experiments

In 10 cm^2 plates, HUVEC conditioned media was generated after one week of HAART drug treatment by washing with PBS and then incubating for 24 hours with complete human astrocyte media. Conditioned media was centrifuged for 5 min at max speed to remove debris and volumes were adjusted according to cell counts. Conditioned media was applied to human astrocytes over the course of one week with a second treatment after 3 days. Senescence-associated β-galactosidase and flow cytometry assays were then performed as described above.

2.12. Statistical analysis

Data were either compared using a two-tailed Student's T-test when 2 groups were involved or one-way analysis of variance (ANOVA) followed by Bonferroni correction when 3 groups were analyzed. Means were derived from at least 3 independent experiments. Error bars on graphs reflect standard deviation (S.D.). Statistical significance was considered at $p < 0.05$.

3. Results

3.1. HAART drugs induce senescence program and inflammatory response in HUVECs

We first treated HUVECs, a type of endothelial cell which has been used in BBB studies (Akiyama et al., 2000; Bang et al., 2017), for one week with physiologically relevant (Nacarelli et al., 2016) amounts of NRTIs commonly used in the clinic, TDF and FTC. Treated cells had a large reduction in proliferative capacity as indicated by reduced cell counts and population doublings over the course of a week (Fig. 1A, B). HAART drug treatment also significantly increased SA-β-Gal positive cells (Fig. 1C). As SA-β-Gal is a reflection of increased lysosomal mass in senescent cells, we wanted to confirm this increase. TDF-FTC treatment significantly increased lysosomal mass, suggesting that it can be used as another indicator of senescence (Fig. 1D). Western blot revealed that protein levels of the nuclear envelope protein lamin B1 decreased (Fig. 1E), an indicator of senescence (Freund et al., 2012).

High mobility group proteins are a class of nonhistone chromatin bound proteins that regulate transcription. The decrease of one such protein, HMGB2, is associated with senescence (Biniossek et al., 2013) and HUVECs treated with TDF-FTC also had decreased levels of this protein (Fig. 2A). Analysis via immunofluorescence microscopy suggest that the decrease observed by western blot could be due to secretion as a higher percentage of HAART drug treated HUVECs appeared to be secreting this protein (Fig. 2B, C). These results support our recent studies demonstrating that circulating levels of HMGB2 increase with age and correlate with neurological functional status (Lawrence et al., 2018).

Next, we examined other secretory effects of HAART-mediated HUVEC senescence by analysis of the senescence associated secretory phenotype (SASP). CM from senescent HUVECs were probed on a cytokine array as previously described with human astrocytes (Cohen et al., 2017). There was a large increase in pro-inflammatory cytokines and chemokines in CM of TDF-FTC treated HUVECs compared to controls (Fig. 3A, Table 1). Some of these cytokines include IL-1α, IL-1β and IL-6 which is particularly interesting as they have been shown to induce senescence in neighboring cells in a paracrine manner (Acosta et al., 2013). In order to validate these results, we performed an ELISA for IL-6 and IL-8, two cytokines that are classically associated with the SASP. Both cytokines significantly increased in CM from HAART drug treated HUVECs (Fig. 3B, C). NF-κB (p65), a pro-inflammatory transcription factor which has been shown to mechanistically induce senescence and the SASP (Freund et al., 2011; Tilstra et al., 2012) is activated as well, suggesting that p65 may regulate HAART drug mediated HUVEC senescence (Fig. 3D). Overall, these results indicate that HAART drugs are able to induce the senescence program in HUVECs.

3.2. HAART drugs induce oxidative stress in HUVECs

Inflammation and ROS have a tightly linked relationship. Since oxidative stress from ROS can induce premature senescence (Chen et al., 1995), we wanted to examine if HUVECs showed signs of oxidative stress with HAART drug-mediated senescence. Total cellular ROS significantly increased in TDF-FTC treated HUVECs (Fig. 4A), indicating oxidative stress.

Since oxidative stress can originate in the mitochondria (Wang et al., 2013), we looked at superoxide anion, a ROS specific to the mitochondria. This mitochondrial ROS significantly increased as well in response to TDF-FTC (Fig. 4B). These results indicate that HUVECs experience oxidative stress in response to HAART drugs.

3.3. Limited effect of p38MAPK inhibition on HUVECs

Since p38MAPK inhibition ameliorated senescence and stress phenotypes across various cell types (Bhat et al., 2012; Freund et al., 2011) we next examined if inhibition affects HAART drug-mediated senescence and stress responses in HUVECs. Promisingly, the HAART drug mediated increase in lysosomal mass that is expected in senescent cells was attenuated by p38MAPK inhibition (Fig. 5A), suggesting that senescence is being ameliorated. However, inhibition did not prevent increases in ROS (Fig. 5B, C), suggesting that oxidative stress in HAART drug treated HUVECs may be independent of p38MAPK and senescence.

3.4. HAART-induced senescence impact HUVEC function

We next wanted to determine if senescent HUVECs have altered physiological function. One key property of endothelial cells is the production of nitric oxide (NO), a free radical signaling molecule that regulates blood pressure (Forstermann and Sessa, 2012). In order to examine this functionality, we evaluated phosphorylation of endothelial nitric oxide synthase (eNOS), the enzyme involved in NO synthesis. ATP was included in these experiments as an inducer of eNOS phosphorylation (Ulker et al., 2018). TDF-FTC significantly decreased ATP-mediated eNOS phosphorylation, suggesting that HAART drugs can inhibit eNOS activation (Fig. 6A, B). To see if this change in eNOS correspond to changes in NO production, we measured intracellular NO. Surprisingly, NO increased with TDF-FTC treatment (Fig. 6C), suggesting that there could be alternative sources of NO production in senescent HUVECs.

Lastly, we wanted to evaluate how endothelial cell senescence can functionally affect other components of the BBB. Since astrocytes maintain contact with endothelial cells in the BBB, we examined the effect of conditioned medium (CM) from HUVECs on astrocytes. First, it was determined if CM would have any senescence inducing effect by looking at SA Beta Gal. Intriguingly, CM from TDF-FTC-induced senescence HUVECs significantly increased SA Beta Gal positive astrocytes (Fig. 7A, B). Importantly, CM from treated HUVECs significantly increased both total and mitochondrial ROS (Fig. 7C, D). Overall, these results suggest that HAART drug-mediated HUVEC senescence can have a detrimental effect on neighboring cells and have major implications for HAND.

Discussion

The HIV-infected population is growing older with a larger risk for age-associated disease (Niccoli and Partridge, 2012). Neurological issues are particularly troubling because even though HAART has decreased the prevalence of the more severe forms of HAND, the milder forms still remain. We have hypothesized that one possible contributor to HAND is the premature induction of cellular senescence at the BBB from exposure to HAART drugs.

Our study provides evidence for this hypothesis by demonstrating that the NRTIs TDF and FTC induce the senescence program, oxidative stress and functional changes in HUVECs.

Due to the importance of the BBB to CNS health and its association with important glial cells such as astrocytes, we examined HAART drug induced endothelial cell senescence as an influencer of HAND. Our results are comparable to studies of HAART drugs on other cell types (Hernandez-Vallejo et al., 2013; Nacarelli et al., 2016) with the induction of classical senescence markers and oxidative stress. However, while it reduced the increased lysosomal mass associated with senescence, p38MAPK inhibition did not decrease ROS in HUVECs, suggesting a divergence in the mechanisms of HAART drug mediated oxidative stress.

HMGB2 has been shown to be involved in reducing heterochromaticity of gene regions associated with the SASP (Aird et al., 2016). Since our TDF-FTC treated HUVECs had a large SASP response, we were curious about HMGB2 localization in our cells. Our data shows that although HMGB2 maintains nuclear and cytoplasmic localization, HAART drug treatment results in secretion of this protein. This increased secretion could have implications for HAND because serum HMGB2 levels correlate with neurological impairment (Lawrence et al., 2018).

In terms of the HUVEC SASP response itself, the largest change in secretion was the FMS-like tyrosine kinase 3 (FIT-3) ligand. This ligand is a small molecule with pro-inflammatory properties induced by binding to CD135, activating hematopoietic progenitors for the production of B and T-Cells (Shortman and Naik, 2007). While there have not been reports examining the relationship between FIT-3 ligand and HAND, there is a potential pro-inflammatory impact of this molecule on the CNS.

HAART drug mediated HUVEC senescence also resulted in changes to physiological function. The eNOS enzyme which regulates blood pressure has both decreased activation and overall expression in response to treatment. Surprisingly, the intracellular levels of the NO molecule produced by this enzyme increased with treatment. There are a couple explanations for this discrepancy, one being that the increased NO levels could be due to impaired secretion. Indeed, ATP, which activates eNOS, decreases intracellular NO which would not be expected with activation unless secreted. Alternatively, our TDF-FTC treatment is inhibiting eNOS mediated NO production, but generation happens from an alternative enzyme. In fact, the endothelium-dependent, cytochrome P450 reductase can compensate for NO deficiency and produce NO from nitrates when needed (Zhao et al., 2015). The role of NO dysfunction in HAND should be further explored as NO dysregulation is not only associated with cardiovascular disease but also neurodegeneration (Forstermann and Sessa, 2012).

Lastly, we examined paracrine effects of HAART drug treated HUVECs on human astrocytes in order to explore how senescence of the BBB could affect the CNS. Most notably, CM from senescent HUVECs induced astrocyte senescence, which implicates that the senescent astrocytes could influence other cells deeper into the CNS. Overall, these results indicate that HAART drugs induce oxidative stress, mitochondrial stress and

senescence in HUVECs. These senescent HUVECs have both eNOS downregulation and paracrine effects which, if mimicked in brain endothelial cells, could be a contributor to HAND. One caveat to our results is that there are other HIV-associated inducers of cellular senescence that could contribute to co-morbidities including the HIV virus itself and its gene products as well as drugs of abuse (Cohen and Torres, 2017). However, it is likely that no one factor is solely responsible and HAART-induced cellular senescence could still be a contributor. Accordingly, clinical trial studies have demonstrated that drugs with greater CNS penetration resulted in impaired neurocognitive performance, despite HIV suppression (Marra et al., 2009), and that in HIV-infected patients with preserved immune function, neurocognitive deficits improved after interruption of HAART treatment (Robertson et al., 2010). These results suggest that HAART drugs could still be a major factor in the development of HAND. Although the use of HUVECs instead of brain microvascular endothelial cells (BMECs) may limits the scope of conclusions, HUVECs have successfully been used in models of the BBB (Akiyama et al., 2000; Bang et al., 2017). Future studies should examine if these results can be mimicked in BMECs in order to extend its clinical relevance.

In conclusion, our data demonstrates that HUVECs undergo premature senescence by the NRTIs TDF and FTC. This senescence is associated with inflammation, oxidative stress, functional disruption and paracrine effects. These data imply that if similar results are found in BMECs, HAART drugs could induce premature senescence at the BBB, which could be a factor for HAND. Changes in ROS and inflammation associated with senescence of HUVECs, support the intervention of the senescence program as target for therapeutics aimed to mitigate HAND.

Acknowledgments

References

Acosta JC, Banito A, Wuestefeld T, Georgilis A, Janich P, Morton JP, Athineos D, Kang TW, Lasitschka F, Andrulis M, et al. (2013). A complex secretory program orchestrated by the inflammasome controls paracrine senescence. Nature cell biology 15, 978–990. [PubMed: 23770676]

Afonso P, Auclair M, Boccara F, Vantyghem MC, Katlama C, Capeau J, Vigouroux C, and Caron-Debarle M (2015). LMNA mutations resulting in lipodystrophy and HIV protease inhibitors trigger vascular smooth muscle cell senescence and calcification: Role of ZMPSTE24 downregulation. Atherosclerosis 245, 200–211. [PubMed: 26724531]

Afonso P, Auclair M, Caron-Debarle M, and Capeau J (2017). Impact of CCR5, integrase and protease inhibitors on human endothelial cell function, stress, inflammation and senescence. Antiviral therapy 22, 645–657. [PubMed: 28350300]

Aird KM, Iwasaki O, Kossenkov AV, Tanizawa H, Fatkhutdinov N, Bitler BG, Le L, Alicea G, Yang TL, Johnson FB, et al. (2016). HMGB2 orchestrates the chromatin landscape of senescence-associated secretory phenotype gene loci. The Journal of cell biology 215, 325–334. [PubMed: 27799366]

Akay C, Cooper M, Odeleye A, Jensen BK, White MG, Vassoler F, Gannon PJ, Mankowski J, Dorsey JL, Buch AM, et al. (2014). Antiretroviral drugs induce oxidative stress and neuronal damage in the central nervous system. Journal of neurovirology 20, 39–53. [PubMed: 24420448]

Akiyama H, Kondoh T, Kokunai T, Nagashima T, Saito N, and Tamaki N (2000). Blood-brain barrier formation of grafted human umbilical vein endothelial cells in athymic mouse brain. Brain research 858, 172–176. [PubMed: 10700611]

Auclair M, Afonso P, Capel E, Caron-Debarle M, and Capeau J (2014). Impact of darunavir, atazanavir and lopinavir boosted with ritonavir on cultured human endothelial cells: beneficial effect of pravastatin. Antiviral therapy 19, 773–782. [PubMed: 24535489]

Bang S, Lee SR, Ko J, Son K, Tahk D, Ahn J, Im C, and Jeon NL (2017). A Low Permeability Microfluidic Blood-Brain Barrier Platform with Direct Contact between Perfusable Vascular Network and Astrocytes. Sci Rep 7, 8083. [PubMed: 28808270]

Bhat R, Crowe EP, Bitto A, Moh M, Katsetos CD, Garcia FU, Johnson FB, Trojanowski JQ, Sell C, and Torres C (2012). Astrocyte senescence as a component of Alzheimer's disease. PloS one 7, e45069. [PubMed: 22984612]

Bhatia R, Ryscavage P, and Taiwo B (2012). Accelerated aging and human immunodeficiency virus infection: emerging challenges of growing older in the era of successful antiretroviral therapy. Journal of neurovirology 18, 247–255. [PubMed: 22205585]

Biniossek ML, Lechel A, Rudolph KL, Martens UM, and Zimmermann S (2013). Quantitative proteomic profiling of tumor cell response to telomere dysfunction using isotope-coded protein labeling (ICPL) reveals interaction network of candidate senescence markers. J Proteomics 91, 515–535. [PubMed: 23969227]

Capeau J (2011). Premature Aging and Premature Age-Related Comorbidities in HIV-Infected Patients: Facts and Hypotheses. Clinical infectious diseases : an official publication of the Infectious Diseases Society of America 53, 1127–1129. [PubMed: 21998279]

Caron M, Auclairt M, Vissian A, Vigouroux C, and Capeau J (2008). Contribution of mitochondrial dysfunction and oxidative stress to cellular premature senescence induced by antiretroviral thymidine analogues. Antiviral therapy 13, 27–38. [PubMed: 18389896]

Chen Q, Fischer A, Reagan JD, Yan LJ, and Ames BN (1995). Oxidative DNA damage and senescence of human diploid fibroblast cells. Proceedings of the National Academy of Sciences of the United States of America 92, 4337–4341. [PubMed: 7753808]

Chinta SJ, Woods G, Demaria M, Rane A, Zou Y, McQuade A, Rajagopalan S, Limbad C, Madden DT, Campisi J, et al. (2018). Cellular Senescence Is Induced by the Environmental Neurotoxin Paraquat and Contributes to Neuropathology Linked to Parkinson's Disease. Cell reports 22, 930–940. [PubMed: 29386135]

Cohen J, D'Agostino L, Wilson J, Tuzer F, and Torres C (2017). Astrocyte Senescence and Metabolic Changes in Response to HIV Antiretroviral Therapy Drugs. Front Aging Neurosci 9, 281. [PubMed: 28900395]

Cohen J, and Torres C (2017). HIV-associated cellular senescence: A contributor to accelerated aging. Ageing research reviews 36, 117–124. [PubMed: 28017881]

Correale J, and Villa A (2009). Cellular elements of the blood-brain barrier. Neurochemical research 34, 2067–2077. [PubMed: 19856206]

Dimri GP, Lee X, Basile G, Acosta M, Scott G, Roskelley C, Medrano EE, Linskens M, Rubelj I, Pereira-Smith O, et al. (1995). A biomarker that identifies senescent human cells in culture and in aging skin in vivo. Proceedings of the National Academy of Sciences of the United States of America 92, 9363–9367. [PubMed: 7568133]

Effros RB, Fletcher CV, Gebo K, Halter JB, Hazzard WR, Horne FM, Huebner RE, Janoff EN, Justice AC, Kuritzkes D, et al. (2008). Aging and infectious diseases: workshop on HIV infection and aging: what is known and future research directions. Clinical infectious diseases an official publication of the Infectious Diseases Society of America 47, 542–553.

Forstermann U, and Sessa WC (2012). Nitric oxide synthases: regulation and function. Eur Heart J 33, 829–837, 837a–837d. [PubMed: 21890489]

Freund A, Laberge RM, Demaria M, and Campisi J (2012). Lamin B1 loss is a senescence-associated biomarker. Mol Biol Cell 23, 2066–2075. [PubMed: 22496421]

Freund A, Patil CK, and Campisi J (2011). p38MAPK is a novel DNA damage response-independent regulator of the senescence-associated secretory phenotype. The EMBO journal 30, 1536–1548. [PubMed: 21399611]

Heaton RK, Clifford DB, Franklin DR, Jr., Woods SP, Ake C, Vaida F, Ellis RJ, Letendre SL, Marcotte TD, Atkinson JH, et al. (2010). HIV-associated neurocognitive disorders persist in the era of potent antiretroviral therapy: CHARTER Study. Neurology 75, 2087–2096. [PubMed: 21135382]

Hernandez-Vallejo SJ, Beaupere C, Larghero J, Capeau J, and Lagathu C (2013). HIV protease inhibitors induce senescence and alter osteoblastic potential of human bone marrow mesenchymal stem cells: beneficial effect of pravastatin. Aging cell 12, 955–965. [PubMed: 23795945]

Hijmans JG, Stockleman K, Reiakvam W, Levy MV, Brewster LM, Bammert TD, Greiner JJ, Connick E, and DeSouza CA (2018). Effects of HIV-1 gp120 and tat on endothelial cell senescence and senescence-associated microRNAs. Physiol Rep 6, e13647. [PubMed: 29595877]

Jeyapalan JC, and Sedivy JM (2008). Cellular senescence and organismal aging. Mechanisms of ageing and development 129, 467–474. [PubMed: 18502472]

Khan SY, Awad EM, Oszwald A, Mayr M, Yin X, Waltenberger B, Stuppner H, Lipovac M, Uhrin P, and Breuss JM (2017). Premature senescence of endothelial cells upon chronic exposure to TNFalpha can be prevented by N-acetyl cysteine and plumericin. Sci Rep 7, 39501. [PubMed: 28045034]

Lawrence I, Bene M, Nacarelli T, Azar A, Cohen JZ, Torres C, Johannes G, and Sell C (2018). Correlations between age, functional status, and the senescence-associated proteins HMGB2 and p16(INK4a). Geroscience

Marra CM, Zhao Y, Clifford DB, Letendre S, Evans S, Henry K, Ellis RJ, Rodriguez B, Coombs RW, Schifitto G, et al. (2009). Impact of combination antiretroviral therapy on cerebrospinal fluid HIV RNA and neurocognitive performance. Aids 23, 1359–1366. [PubMed: 19424052]

Munoz-Espin D, and Serrano M (2014). Cellular senescence: from physiology to pathology. Nat Rev Mol Cell Biol 15, 482–496. [PubMed: 24954210]

Nacarelli T, Azar A, and Sell C (2016). Mitochondrial stress induces cellular senescence in an mTORC1-dependent manner. Free Radic Biol Med 95, 133–154. [PubMed: 27016071]

Negredo E, Back D, Blanco JR, Blanco J, Erlandson KM, Garolera M, Guaraldi G, Mallon P, Molto J, Serra JA, et al. (2017). Aging in HIV-Infected Subjects: A New Scenario and a New View. Biomed Res Int 2017, 5897298. [PubMed: 29430462]

Niccoli T, and Partridge L (2012). Ageing as a risk factor for disease. Curr Biol 22, R741–752. [PubMed: 22975005]

Robertson KR, Su Z, Margolis DM, Krambrink A, Havlir DV, Evans S, Skiest DJ, and Team AS (2010). Neurocognitive effects of treatment interruption in stable HIV-positive patients in an observational cohort. Neurology 74, 1260–1266. [PubMed: 20237308]

Rojas M, Lemtalsi T, Toque HA, Xu Z, Fulton D, Caldwell RW, and Caldwell RB (2017). NOX2-Induced Activation of Arginase and Diabetes-Induced Retinal Endothelial Cell Senescence. Antioxidants (Basel) 6.

Saylor D, Dickens AM, Sacktor N, Haughey N, Slusher B, Pletnikov M, Mankowski JL, Brown A, Volsky DJ, and McArthur JC (2016). HIV-associated neurocognitive disorder--pathogenesis and prospects for treatment. Nat Rev Neurol 12, 234–248. [PubMed: 26965674]

Shortman K, and Naik SH (2007). Steady-state and inflammatory dendritic-cell development. Nat Rev Immunol 7, 19–30. [PubMed: 17170756]

Tilstra JS, Robinson AR, Wang J, Gregg SQ, Clauson CL, Reay DP, Nasto LA, St Croix CM, Usas A, Vo N, et al. (2012). NF-kappaB inhibition delays DNA damage-induced senescence and aging in mice. The Journal of clinical investigation 122, 2601–2612. [PubMed: 22706308]

Turnquist C, Horikawa I, Foran E, Major EO, Vojtesek B, Lane DP, Lu X, Harris BT, and Harris CC (2016). p53 isoforms regulate astrocyte-mediated neuroprotection and neurodegeneration. Cell Death Differ 23, 1515–1528. [PubMed: 27104929]

Ulker P, Ozen N, Abdullayeva G, Koksoy S, Yaras N, and Basrali F (2018). Extracellular ATP activates eNOS and increases intracellular NO generation in Red Blood Cells. Clin Hemorheol Microcirc 68, 89–101. [PubMed: 29036803]

van Deursen JM (2014). The role of senescent cells in ageing. Nature 509, 439–446. [PubMed: 24848057]

Wang CH, Wu SB, Wu YT, and Wei YH (2013). Oxidative stress response elicited by mitochondrial dysfunction: implication in the pathophysiology of aging. Experimental biology and medicine 238, 450–460. [PubMed: 23856898]

Zhao Y, Vanhoutte PM, and Leung SW (2015). Vascular nitric oxide: Beyond eNOS. J Pharmacol Sci 129, 83–94. [PubMed: 26499181]

Highlights

- The NRTIs TDF and FTC induce premature senescence in HUVECs

- Senescent HUVECs possess an inflammatory response and oxidative stress

- Senescent HUVECs have altered eNOS activation

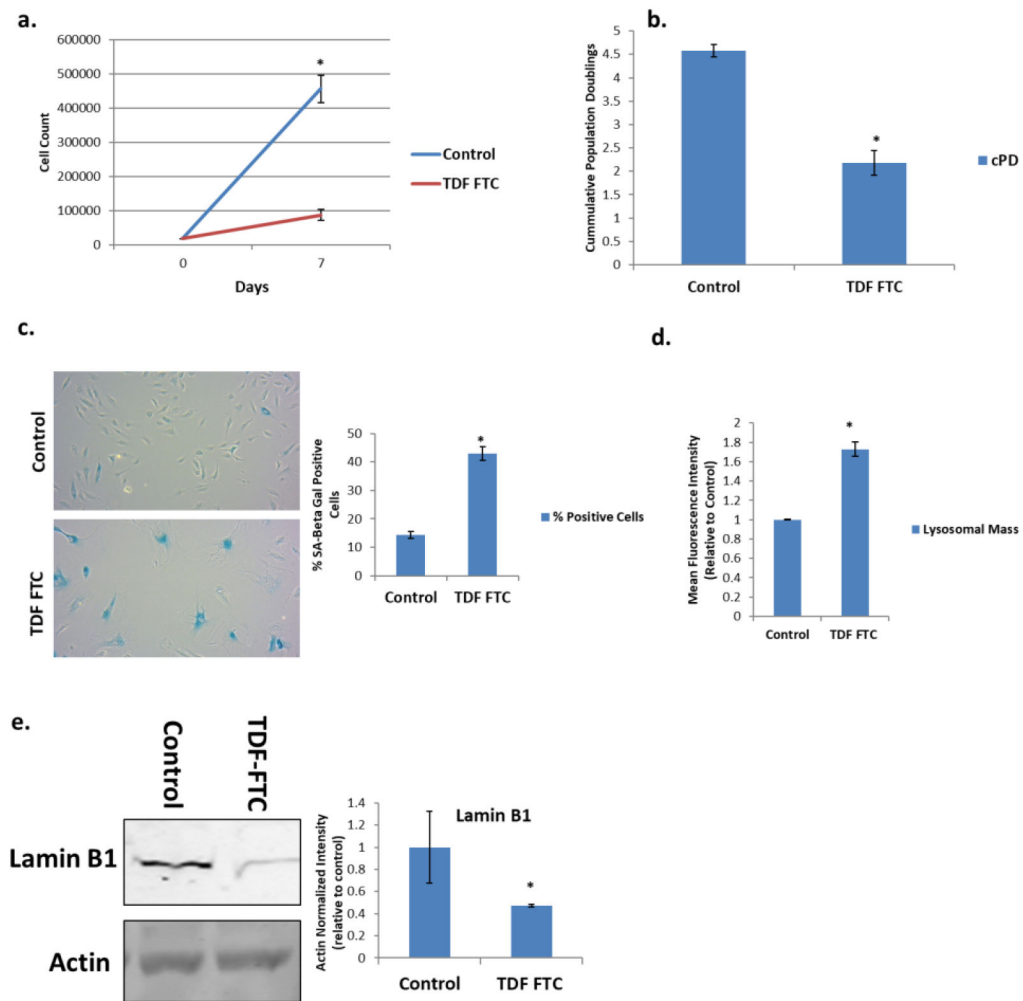- Senescent HUVEC conditioned media induces premature senescence in astrocytes

Figure 1. Expression of Senescence Markers in HAART Drug Treated HUVECs.

HUVECs were treated with 10 μg/mL of tenofovir (TDF) and emtricitibine (FTC) for 7 days. **(A)** Growth curve. **(B)** Population doublings over one week. **(C)** *Left*, representative SA β-gal images displayed at 20X of human astrocytes stained for SA β-gal 1 week after HAART treatment. *Right*, quantification of images. **(D)** Lysosomal mass was measured by incubation with Lysotracker for 30 min followed by quantification on a flow cytometer. **(E)** *Left*, representative western blot of senescence markers lamin B1 and loading control. *Right*, quantification. * = p value < .05, n = 3, error bars are S.D.
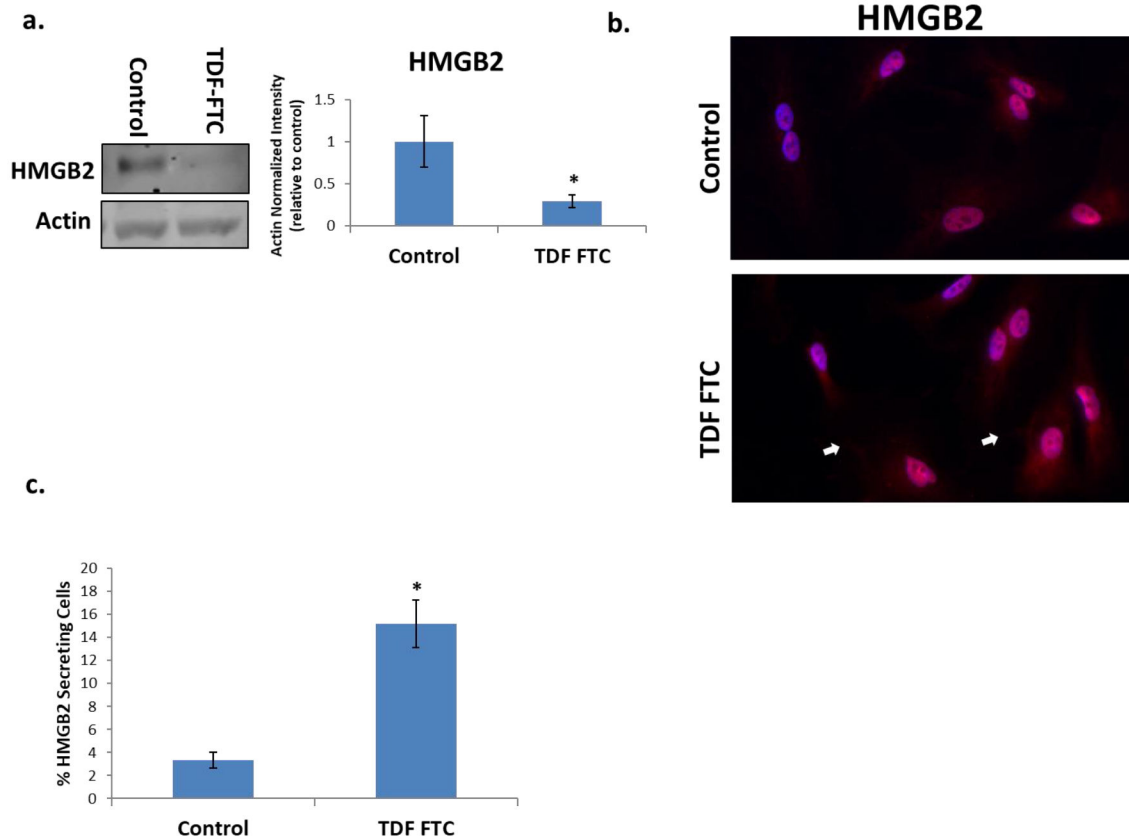
Figure 2. Effect of HAART Drugs on HMGB2 in HUVECs.
HUVECs were treated with 10 μg/mL of tenofovir (TDF) and emtricitibine (FTC) for 7 days. **(A)** *Left*, representative western blot of HMGB2 and loading control. *Right*, quantification. **(B)** Microscopy of HMGB2 at 40X. White arrows point to tendrils of secreted HMGB2. **(C)** Quantification of B, at least 200 cells per well were counted. * = p value < .05, n = 3, error bars are S.D.
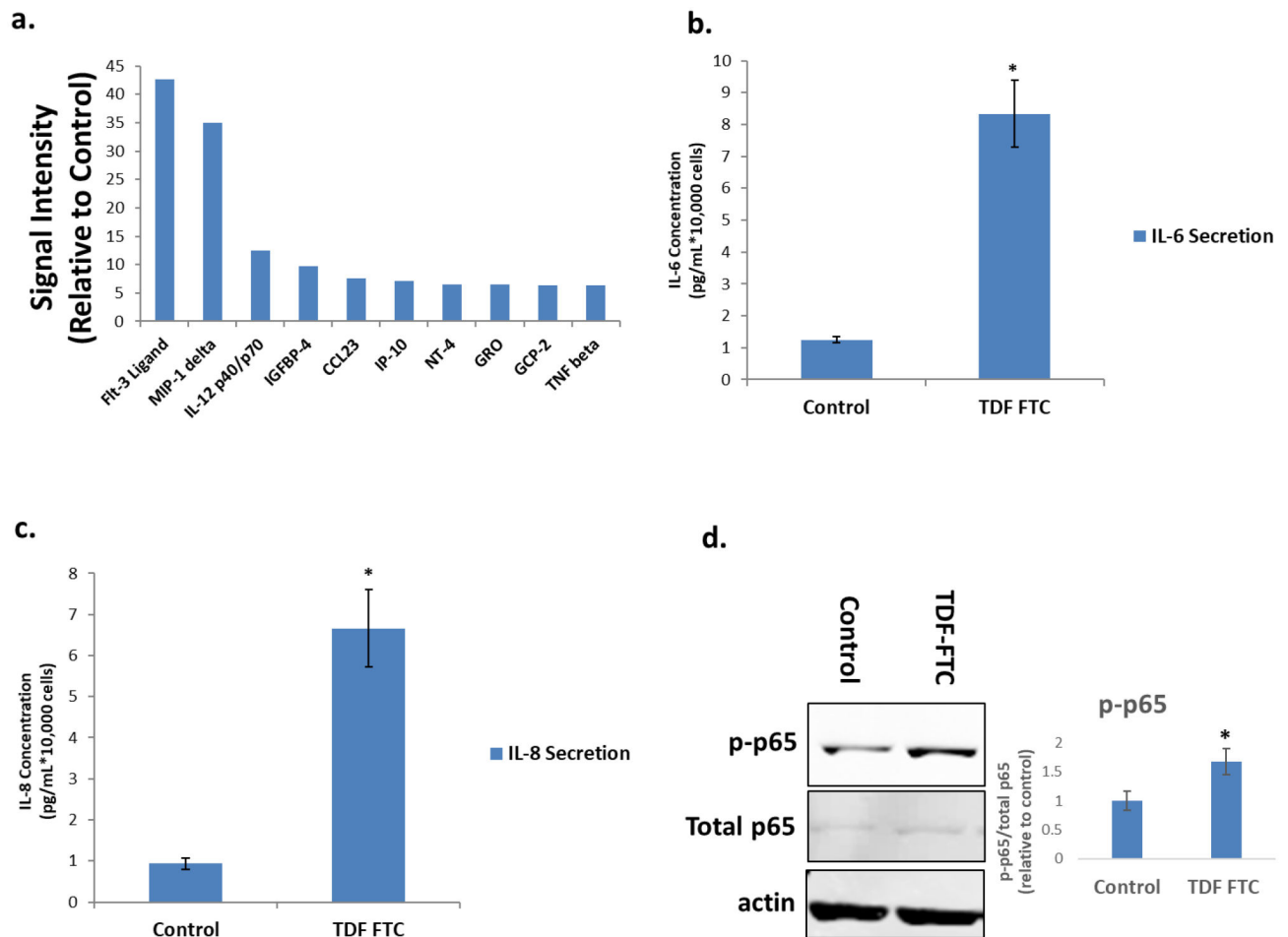
Figure 3. Secretory profile of HAART Drug Treated HUVECs.

HUVECs were treated with 10 μg/mL of tenofovir (TDF) and emtricitibine (FTC) for 7 days. **(A)** Senescence-associated secretory phenotype (SASP) analysis. After antiretroviral treatment, HUVECs were subjected to a 24-hour incubation in MCBD105 media to generate conditioned media (CM). The secretory profile was detected by incubating CM on a cytokine membrane array and normalized to cell number. Values are relative to a vehicle control. **(B)** IL-6 quantitation. CM was collected as in A and IL-6 was quantitated by ELISA. **(C)** IL-8 quantitation. CM was collected as in A and IL-8 was quantitated by ELISA. **(D)** *Left*, representative western blot illustrating protein levels of inflammatory mediator p65and loading control. *Right*, quantification. * = p value < .05, n = 3, error bars are S.D.
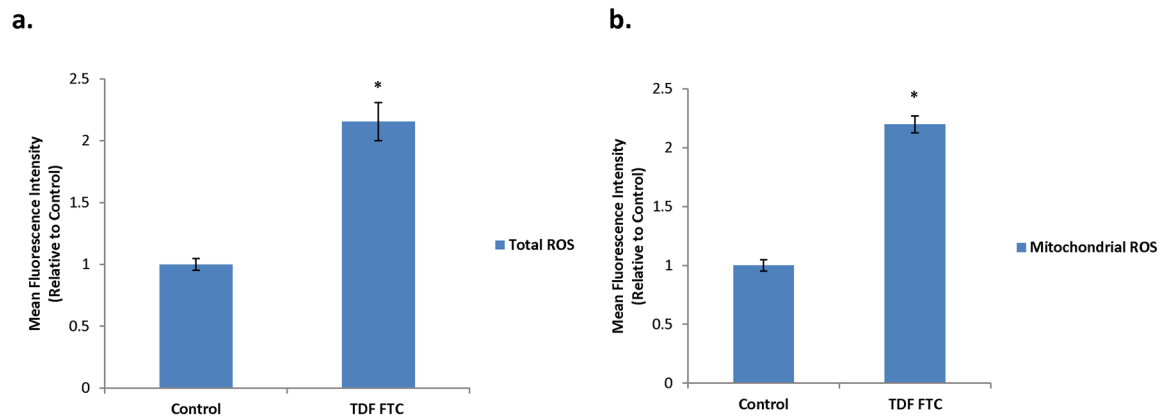
a.

b.

Figure 4. Increased Oxidative Stress in HAART Drug Treated HUVECs.
HUVECs were treated with 10 μg/mL of tenofovir (TDF) and emtricitibine (FTC) for 7 days. **(A)** Total ROS was measured by incubation with DCFDA for 30 min followed by quantification on a flow cytometer. **(B)** Mitochondrial ROS was measured by incubation with MitoSox for 30 min followed by quantification on a flow cytometer. * = p value < .05, n = 3, error bars are S.D.
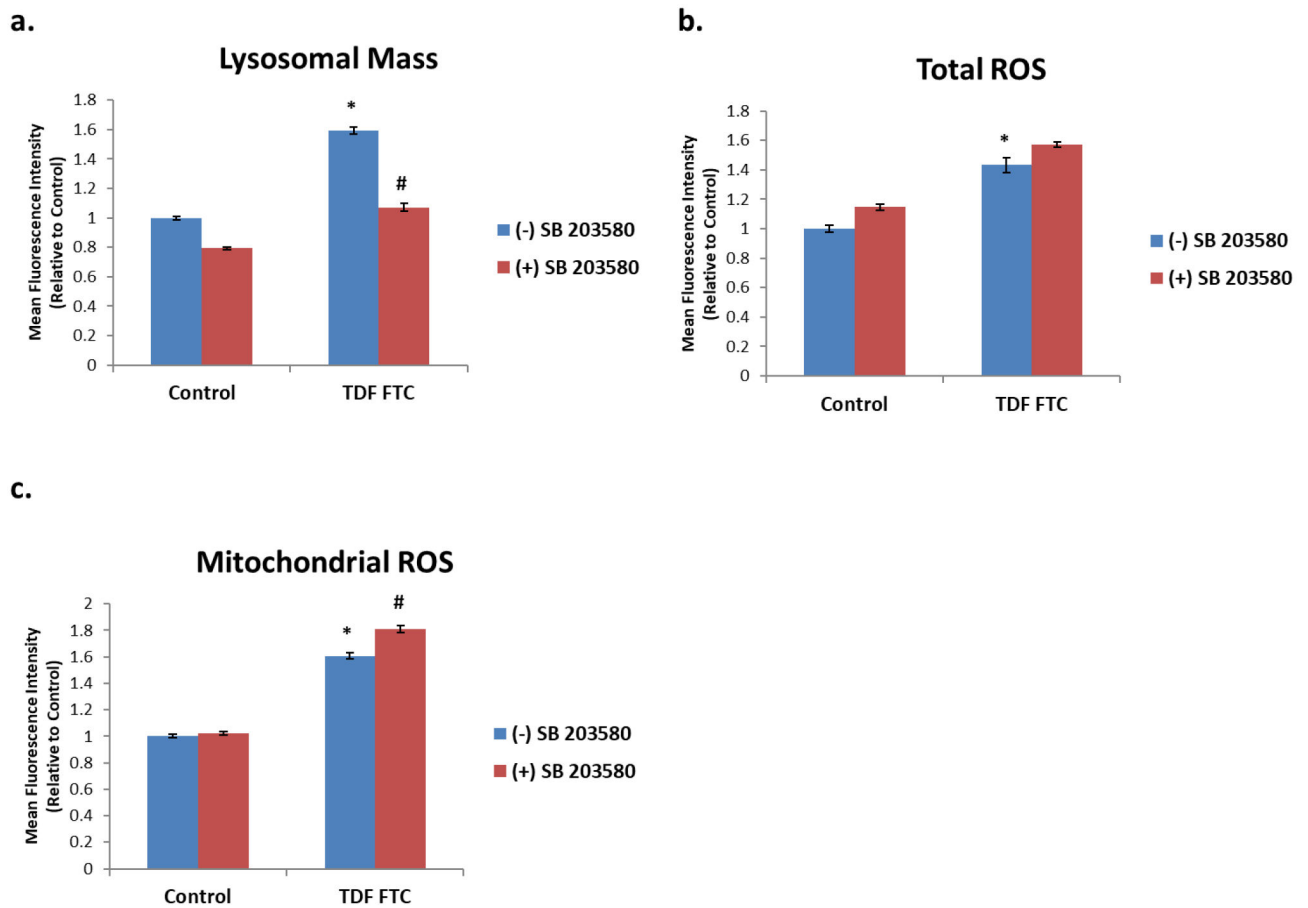
Figure 5. Effect of p38MAPK Inhibition on HAART Drug Treated HUVECs.
HUVECs were treated with 10 μg/mL of tenofovir (TDF) and emtricitibine (FTC) for 7 days. Where indicated, cells were pre-treated with 10 μM SB 203580 for 2 hours prior to HAART drug addition. **(A)** Lysosomal mass was measured by incubation with Lysotracker for 30 min followed by quantification on a flow cytometer. **(B)** Total ROS was measured by incubation with DCFDA for 30 min followed by quantification on a flow cytometer. **(C)** Mitochondrial ROS was measured by incubation with MitoSox for 30 min followed by quantification on a flow cytometer. * = p value < .05, n = 3, error bars are S.D.
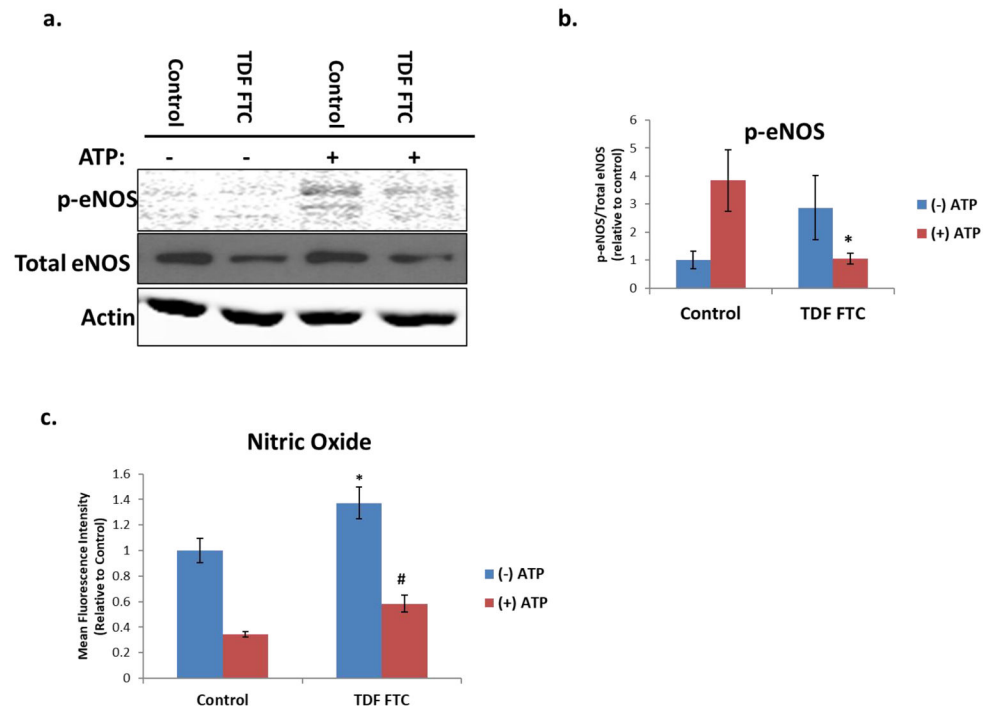
Figure 6. Nitric Oxide Activity in HAART Drug Treated HUVECs.
HUVECs were treated with 10 μg/mL of tenofovir (TDF) and emtricitibine (FTC) for 7 days. Where indicated, cells were treated with 100 μM ATP one minute prior to collection. **(A)** Protein levels of p-eNOS and total eNOS as measured by western blot. **(B)** Quantification of A. **(C)** Intracellular nitric oxide was measured by incubation with DAF-FM and ATP for 30 min followed by a PBS wash and 15 min incubation before quantification on a flow cytometer. *= p value < .05 compared to (−) ATP control, # = p value < .05 compared to (−) ATP TDF FTC, n = 3, error bars are S.D.
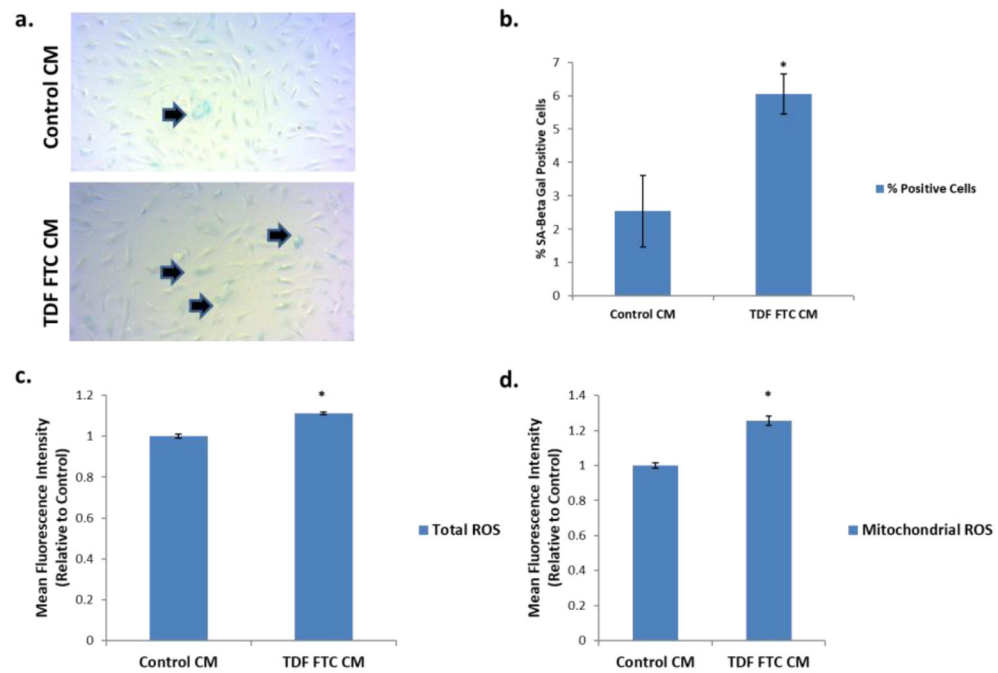
Figure 7. Effect of HUVEC Conditioned Media on Human Astrocytes.
HUVECs were treated with 10 μg/mL of tenofovir (TDF) and emtricitibine (FTC) for 7 days. Cells were then incubated in human astrocyte media (HAM) for 24 hours to generate conditioned media (CM). CM was then incubated on human astrocytes for 7 days before indicated assays. **(A)** Representative SA Beta Gal assay images at 10X. **(B)** Quantification of A. **(C)** Total ROS was measured by incubation with DCFDA for 30 min followed by quantification on a flow cytometer. **(D)** Mitochondrial ROS was measured by incubation with MitoSox for 30 min followed by quantification on a flow cytometer. * = p value < .05, n = 3, error bars are S.D.

Table 1.

Senescence-Associated Secretory Phenotype of TDF-FTC Treated HUVECs.

Cytokines were measured by an antibody array and values are expressed as relative to control.

Name	TDF-FTC	Name cont.	TDF-FTC cont.
Angiogenin	3.292861	LIF	4.444799
BDNF	4.835223	Light	3.200824
BLC	3.950735	MCP-1	4.404267
EGF	4.497927	MCP-2	2.155095
Eotaxin-1	5.544542	MCP-4	3.813051
Eotaxin-2	4.617339	M-CSF	2.910713
Eotaxin-3	5.286011	MDC	5.277246
FGF-4	0	MIF	3.472801
FGF-6	5.404993	MIG	2.880962
FGF-7	2.690579	MIP-1 beta	3.171541
FGF-9	2.679582	MIP-1 delta	34.92573
Flt-3 Ligand	42.58763	MIP-3 alpha	5.964816
Fractalkine	3.120375	NAP-2	4.621764
GCP-2	6.316612	NT-3	4.194772
GDNF	4.015717	NT-4	6.497669
GM-CSF	4.297755	Oncostatin M	4.81561
GRO	6.478263	Osteopontin	5.388738
GRO alpha	5.457758	Osteoprotegerin	1.854735
HGF	2.866196	PARC	1.906955
I-309	0.712365	PDGF-BB	3.002625
IFN-gamma	4.114323	PLGF	1.764793
IGF-1	4.84196	RANTES	2.992735
IGFBP-1	4.430662	SCF	5.807743
IGFBP-2	3.658811	SDF-1	2.176554
IGFBP-3	2.949313	TARC	4.312071
IGFBP-4	9.790448	TGF beta 1	1.618843
IL-1 alpha	1.573047	TGF beta 2	2.943513
IL-1 beta	3.838401	TGF beta 3	5.057033
IL-12p40/p70	12.4681	Thrombopoietin	3.717685
IL-15	4.047189	TIMP-1	3.52869
IL-16	5.903197	TIMP-2	2.980767
IL-2	2.062056	TNF alpha	4.969746
IL-3	3.463601	TNF beta	6.2782
IL-4	3.243654	VEGF-A	2.689809
IL-5	2.076315	CCL23	7.640963
IL-6	5.151946	ENA-78	2.619985

Name	TDF-FTC	Name cont.	TDF-FTC cont.
IL-7	4.194004		
IL-8	4.305946		
IP-10	7.109539		
Leptin	1.683492		

Author Manuscript

Author Manuscript

Author Manuscript

Author Manuscript